International Journal of Mechanical and Electrical Engineering
ISSN: 3005-9615 (Print), ISSN: 3005-7132 (Online) | Volume 4, Number 1, Year 2024
DOI: https://doi.org/10.62051/ijmee.v4n1.02
Journal homepage: https://wepub.org/index.php/IJMEE/index

Study on Aerodynamic Performance of Propeller with Tip Winglet

Yueqi Yang

The High School affiliated Renmin University of China International Cumiculum Center, Beijing 100080, China

ABSTRACT

Based on the Reynolds-averaged Navier-Stokes governing equations and the unstructured grid rotating/stationary sliding surface technology, this paper studies the aerodynamic layout and efficiency enhancement mechanism of the near-space propeller blade tip winglet configuration. First, the feasibility of the configuration is verified by comparing and analyzing different lift propeller layout schemes. Secondly, the aerodynamic layout design of the blade tip winglet propeller is studied by changing the winglet inclination angle and length parameter indicators. Finally, the ANSYS simulation analysis is used to calculate the influence of the winglet design on the propeller velocity vector distribution, blade pressure and propeller aerodynamic efficiency, and the performance influence law of the basic parameters is preliminarily established, and the overall design scheme of the new blade tip winglet propeller design is completed. The study shows that the blade tip winglet propeller layout is a reasonable and feasible technical approach to improve the aerodynamic efficiency in the near-space working environment, and it has a certain reference role in the development of new configuration propeller aircraft.

KEYWORDS

Propeller Tip Winglet; Navier-Stokes Equation; Aerodynamic Performance; Simulation Analysis.

1. INTRODUCTION

The winglet has a similar shape to the wing and is installed at the wingtip, forming a certain angle with the plane of the wing. The installation of the winglet can significantly change the flow field near the wingtip, weaken the wingtip vortex, and reduce the energy consumption directly related to the drag [1] . At the same time, the lateral flow velocity near the vortex center of the wing is significantly reduced, and the downwash of the flow near the wing surface is reduced, which significantly reduces the induced drag of the wing [2] . In the field of aircraft design, there have been many successful application examples since the design concept was proposed, such as KC 135 , Boeing 747, etc. It is reported that the flight test of the US KC 135 aerial refueling aircraft equipped with winglets showed that the aircraft's induced drag can be reduced by 15%, the lift-to-drag ratio can be increased by 5% to 8%, and fuel consumption can be reduced by 9%, and the performance improvement is quite considerable; the "blended winglets" developed by Boeing can reduce aircraft wheel chock fuel consumption by 3% to 5% and reduce airport noise during takeoff by about 6.5 %, with very good results.

For near-space propeller propulsion systems, how to effectively improve propulsion efficiency is a key issue in the development of near-space low-speed aircraft due to the stringent requirements of energy utilization, which seriously affects the overall design, weight, volume and other factors [3] . Therefore, exploring and developing new concepts of efficient propeller layout has important

academic significance and application value. In recent years, inspired by the mechanism of winglets, foreign countries have proposed efficient propeller layout based on winglets. By arranging winglet devices at the propeller tip, the propeller induced drag is reduced, thereby improving aerodynamic efficiency [4] . For example, Irwin K [5] and others applied vortex theory and experimental methods to carry out research on the optimization design of propeller configurations with tip winglets. The experiment showed that: under the same advance ratio, the tip winglet layout can improve the aerodynamic efficiency by about 1%; Purdue University [6] in the United States carried out performance optimization design and experimental verification research on various propeller layouts with tip winglets. The research showed that: the optimal propeller layout scheme improved the efficiency by about 5%; in China, Xu [7] used structured nested grid technology to carry out comparative analysis of various propeller layouts with tip winglets, which improved the aerodynamic efficiency by about 2%.

At present, the research on the propeller layout of blade tip winglets in China is not in-depth enough, and there is a lack of understanding of the mechanism of blade tip winglets and the influence of key parameters. In order to meet the needs of the development of propulsion systems for near-space airships and other aircraft in my country, this paper carried out a study on the propeller layout and efficiency enhancement mechanism of blade tip winglets in near-space working conditions, established the performance influence law of basic parameters, and obtained an efficient layout plan for near-space propellers.

2. THEORETICAL DESCRIPTION

2.1. Governing Equations and Numerical Methods

For the control volume, the integral form of the N -S equation can be expressed as:

$$\iiint_{\Omega} \frac{\partial \boldsymbol{W}}{\partial t} \mathrm{dV} + \iint_{\partial\Omega} \vec{\boldsymbol{H}} \cdot \boldsymbol{n} \mathrm{dS} = \iint_{\partial\Omega} \vec{\boldsymbol{H}}_v \cdot \boldsymbol{n} \mathrm{dS}$$

where W is the state vector, $\vec{\mathrm{H}}$ is the inviscid (convection) flux vector term, $\vec{\mathrm{H}}$v is the viscous (dissipation) flux vector term, and the specific expressions of each term are as follows:

$$\boldsymbol{W} = \begin{bmatrix} \rho \\ \rho u \\ \rho v \\ \rho w \\ \rho E \end{bmatrix}, \vec{\boldsymbol{H}} = \begin{bmatrix} \rho \boldsymbol{q} \\ \rho u \boldsymbol{q} + p \boldsymbol{I}_x \\ \rho v \boldsymbol{q} + p \boldsymbol{I}_y \\ \rho w \boldsymbol{q} + p \boldsymbol{I}_z \\ \rho H \boldsymbol{q} \end{bmatrix}, \vec{\boldsymbol{H}}_v = \begin{bmatrix} 0 \\ \tau_{xx} \boldsymbol{I}_x + \tau_{xy} \boldsymbol{I}_y + \tau_{xz} \boldsymbol{I}_z \\ \tau_{xy} \boldsymbol{I}_x + \tau_{yy} \boldsymbol{I}_y + \tau_{yz} \boldsymbol{I}_z \\ \tau_{xz} \boldsymbol{I}_x + \tau_{zy} \boldsymbol{I}_z + \tau_{zz} \boldsymbol{I}_z \\ \beta_x \boldsymbol{I}_x + \beta_y \boldsymbol{I}_y + \beta_z \boldsymbol{I}_z \end{bmatrix}$$

Among them, $\boldsymbol{q} = (u, v, w)^{\mathrm{T}}$is the fluid velocity vector, $\boldsymbol{I}_x$, $\boldsymbol{I}_y$, $\boldsymbol{I}_z$are the unit coordinate vectors of the rectangular coordinate system, and the physical quantities *ρ, E, H, and p* are density, total energy, total enthalpy, and pressure, respectively.

In addition, the space is discretized using the central average finite volume method, and the time direction is implicitly solved using the dual-time method. In order to accelerate convergence, local time step , implicit residual smoothing, multiple grids and other accelerated convergence measures are adopted .

Since the propeller in this paper works at a low Reynolds number, the turbulence model selected is not the general *k* - *ω* SST model, but simplified *k* - *ε* Model .

This equation was derived directly from the *k* - *ε model* by Menter [5] , so it is also called *the (k* - *ε) 1E* model:

$$\frac{\partial \rho \tilde{v}_t}{\partial t} + \frac{\partial \rho U_j \tilde{v}_t}{\partial x_j} = c_1 \rho \tilde{v}_t S - c_2 \rho (\frac{\tilde{v}_t}{L_{vK}})^2 + (\mu + \frac{\rho \tilde{v}_t}{\sigma}) \frac{\partial \tilde{v}}{\partial x_j}$$

Among them, $\tilde{v}$is the eddy viscosity of motion, $\tilde{v}_t$is the turbulent eddy viscosity, σ is a model constant . The model includes a destruction term that determines the turbulence structure, and the basis of this destruction term is the von Karman scale:

$$(L_{vK})^2 = \left| \frac{S^2}{\frac{\partial S}{\partial x_j} \frac{\partial S}{\partial x_j}} \right|$$

where S is the shear strain rate tensor and the eddy viscosity is calculated by the following formula:

$$\mu_t = \rho \tilde{v}_t$$

In order to prevent the occurrence of singularities in the von Karman length scale, the destruction term is rearranged to obtain:

$$E_{k-\varepsilon} = (\frac{\tilde{v}_t}{L_{vK}})^2$$

$$E_{BG} = \frac{\partial \tilde{\boldsymbol{v}}_t}{\partial x_j} \frac{\partial \tilde{\boldsymbol{v}}_t}{\partial x_j}$$

$$E_{1e} = c_3 E_{BB} \tanh(\frac{E_{k-\varepsilon}}{c_3 E_{BB}})$$

The final result is:

$$\frac{\partial \rho \tilde{v}_t}{\partial t} + \frac{\partial \rho U_j \tilde{v}_t}{\partial x_i} = c_1 D_1 \rho \tilde{v}_t S - c_2 \rho E_{1e} + (\mu + \frac{\rho \tilde{v}_t}{\sigma}) \frac{\partial \tilde{v}_t}{\partial x_i}$$

The low Reynolds number equations for the entire simplified model are achieved by introducing a damping term. The near-wall damping term is developed to allow integration near the wall:

$$D_1 = \frac{v_t + v}{\tilde{v}_t + v}$$

$$D_2 = 1 - \exp\left[-(\frac{\tilde{v}_t}{A + \kappa v})^2\right]$$

where *D2* It is used to calculate the eddy viscosity term in the momentum equation.

$$\mu_t = \rho D_2 \tilde{v}_t$$

The low Reynolds number equation requires a near-wall grid resolution of $y^+ < 1$.

2.2. Computational Grid Model

The working state of the propeller is an unsteady state. In this situation, the entire flow field is divided into two regions: the rotating domain and the stationary domain. As shown in Figure 1, the rotating domain contains the propeller area grid, simulating the flow near the propeller, and the stationary domain is the area outside the rotating domain, simulating the far-field flow. The flow field information is transmitted between the stationary domain and the rotating domain through rotation/static interface interpolation. For the axial flow state, the flow is quasi-steady, and the calculation only needs to be performed on one blade. The influence of other blades is realized through rotational symmetric boundary conditions. Considering the feasibility of mesh division and the calculation accuracy, this paper adopts full-area unstructured mesh division. The mesh density in different regions is different, and the closer to the blade surface, the denser the mesh.

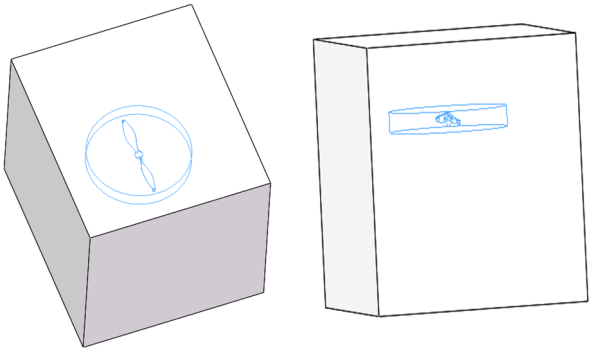

Figure 1. Schematic diagram of simulation flow field division

The blade surface is a triangular grid. In order to simulate the propeller boundary layer flow, 11 layers of prismatic grids are established on the blade surface. The first layer of grid spacing is about 0.005, and the height growth factor of each subsequent layer is 1.2. Other areas are tetrahedral grids, and the total number of grids is about 500,000.

Figure 2. Schematic diagram of grid division

2.3. Efficiency Analysis Method

The aerodynamic efficiency analysis of a propeller is a task involving multiple parameters and complex physical processes. In order to describe this process in general, the following key formulas and concepts are introduced.

First, the ideal efficiency (η) of a propeller is defined as the ratio of the work done by the propeller thrust per unit time (ΔET) to the total work done by the propeller on the airflow (ΔE). Its mathematical expression is:

$$\eta = \Delta ET / \Delta E$$

The work done by the thrust (ΔET) can be calculated by multiplying the thrust (T) of the propeller by the forward speed (V), i.e.:

$$\Delta ET = T \times V$$

The total work (ΔE) done by the propeller on the airflow is mainly reflected in the increase in the kinetic energy of the airflow. In order to simplify the analysis, we usually use some assumptions and approximations, such as assuming that the airflow is uniform before and after the propeller, and the effect of the propeller on the airflow is mainly reflected in the increase in speed. In this case, the total work (ΔE) can be approximately expressed as:

$$\Delta E \approx 1/2 \times \rho \times A \times (V12)$$

Among them, ρ represents the density of air, A is the area swept by the propeller, V1 and V0 are the speeds of the airflow before and after the propeller acts, respectively.

By introducing these formulas and concepts, a preliminary description and evaluation of the propeller's aerodynamic efficiency is made. Subsequent research will further explore the specific effects of these parameters on propeller efficiency and seek effective methods to optimize propeller design.

3. PARAMETRIC ANALYSIS

Referring to the design of the winglet, the propeller tip winglet is realized by adding a winglet configuration to the reference blade. This paper mainly studies the winglet layout. The three-dimensional structure diagram is shown in Figure 3. The propeller winglet is designed by changing the two parameters of winglet length and inclination angle. The parameters are shown in Table 1. The relative position of the winglet is in the outer area of the blade.

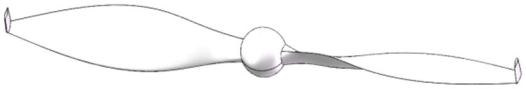

Figure 3. Three-dimensional structure diagram of the new propeller with blade tip wing designed in this paper

Table 1. Propeller design scheme

Plan	Winglet length (mm)	Winglet inclination angle (°)
1	15	45
2	30	45
3	15	90
4	30	90
5 (Control Group)	0	0

The airfoil used in the winglet configuration studied in this paper is a tip profile airfoil. The winglet surface and the blade surface are constructed through multi-section surfaces. To ensure the smoothness of the surface, the restriction condition is curvature continuity.

4. EXAMPLE ANALYSIS

The diameter of the benchmark blade studied in this paper is 0.6 m, working at an altitude of 10 km, with an air density of about 0.41 kg/m³, a rotation speed of 4200 r/min, an incoming wind speed of 15 m/s, an experimental efficiency of 85%, and a calculation efficiency of 80%. The following simulation analysis calculates the influence of the winglet design on the propeller velocity vector distribution and blade pressure. The velocity vector distribution cloud diagram is shown in Figure 4. The speed behind the propeller is higher, indicating that the fluid is accelerated to form a strong thrust under the action of the propeller, and the fluid speed at the edge of the propeller is relatively slow. The velocity vector is used to analyze the flow characteristics of the propeller. The simulation results of the propeller designed in this paper show that the fluid flows smoothly along the propeller blades, reducing vortex and energy loss, and improving efficiency to a certain extent.

The pressure change trend of the propeller blade with the winglet added was calculated. The design with high blade pressure can provide higher lift and thrust, effectively improving the efficiency and performance of the propeller. The larger pressure gradient will lead to stronger fluid acceleration and enhance thrust output. The pressure distribution cloud diagram is shown in Figure 5. The leading

edge area of the propeller has higher pressure and the trailing edge pressure is lower, indicating that the fluid has formed a low-pressure area behind the propeller. The change from the high-pressure area to the low-pressure area on the blade surface forms a larger pressure gradient, which enhances the thrust output, indicating that overall performance has been improved. As shown in the simulation analysis result diagram in Figure 6, when the winglet inclination angle is 90 degrees and the winglet length is 15mm, the maximum blade pressure test effect is better, indicating that the winglet inclination angle and length have a significant effect on the improvement of propeller performance.

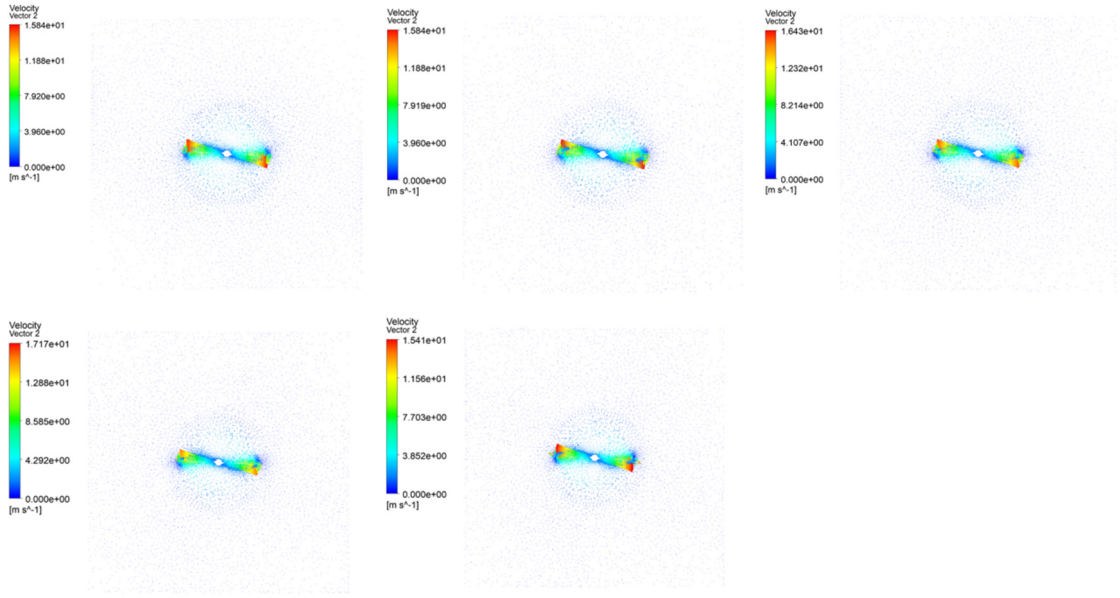

Figure 4. Velocity distribution cloud diagram of simulation test

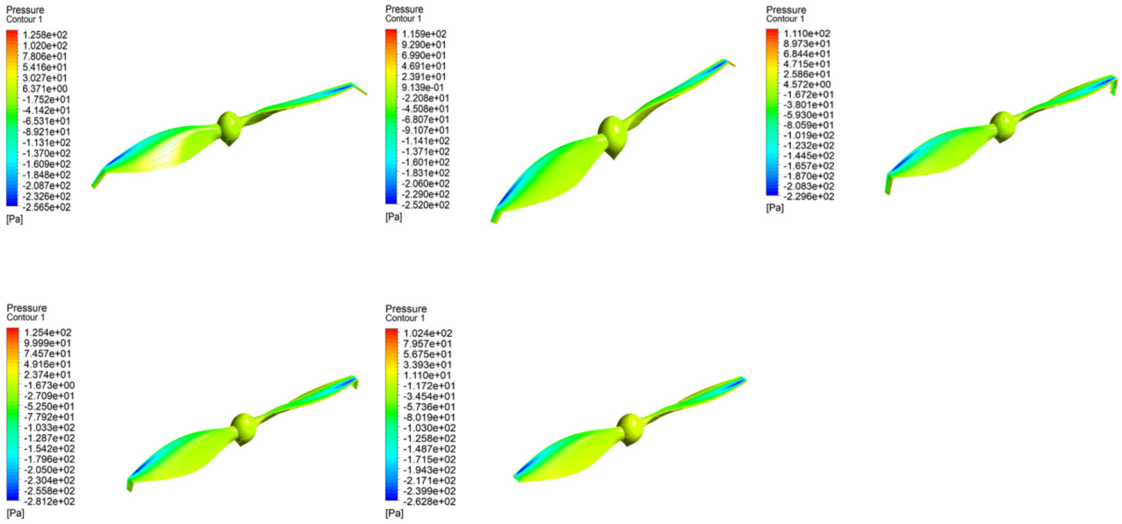

Figure 5. Pressure distribution cloud diagram of simulation test

As shown in Figure 7, the efficiency analysis test results show that the winglet length at different inclination angles significantly affects efficiency performance. At a 45° inclination angle, the 15mm and 30mm winglet lengths increase the efficiency to 86% and 87.4%, respectively, significantly better than the 70.2% of the control group; at a 90° inclination angle, the efficiencies of the 15mm and 30mm winglet lengths are 75.4% and 76.8%, respectively, also higher than the 70.2% of the control group. Overall, the efficiency of the 30mm winglet at both inclination angles is slightly higher than

that of the 15mm winglet, and the efficiency at a 45° inclination angle is significantly better than that at 90°, indicating that lower inclination angles and longer winglets are more conducive to improving efficiency.

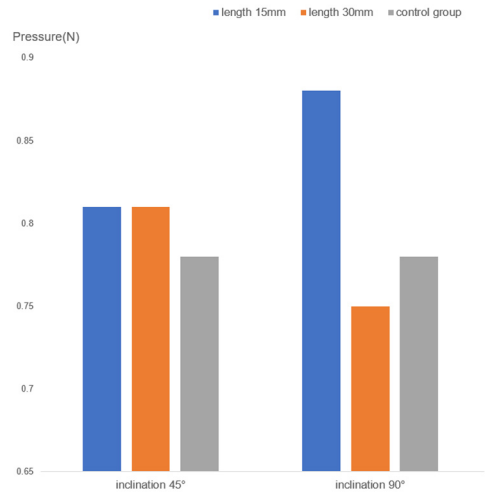

Figure 6. Simulation analysis results

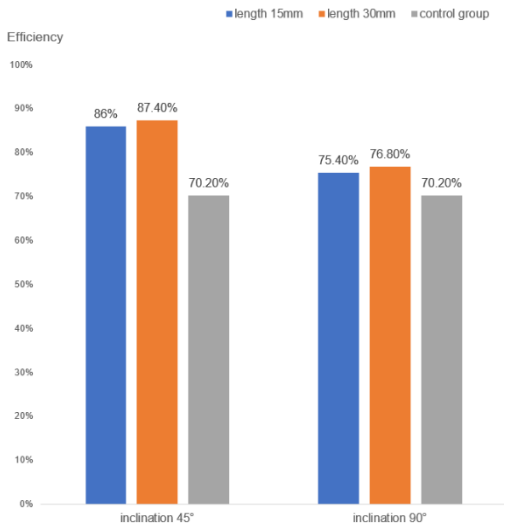

Figure 7. Efficiency analysis results

5. CONCLUSION

By applying a comprehensive analysis method using unstructured grids and Reynolds-averaged Navier-Stokes (RANS) equations, this study designed and evaluated a novel propeller configuration with tip winglets aimed at enhancing aerodynamic performance in near-space conditions. Key findings from the simulation analysis reveal:

1. Significant Influence of Winglet Parameters: Parameters such as winglet length and inclination angle have a critical impact on propeller efficiency. Optimizing these parameters can significantly enhance performance by adjusting the aerodynamic properties at the blade tips.

2. Enhanced Flow Field Distribution: The addition of winglets at the propeller tips alters the flow field distribution, diminishing the wingtip vortex effect and reducing associated drag losses. This

modification allows for improved load distribution across the blade, directly contributing to increased thrust and propeller efficiency.

3.Validated Practicality of Tip Winglet Layout: The study confirms that a propeller layout incorporating tip winglets is a technically viable solution for boosting aerodynamic efficiency in near-space operating environments. This configuration provides a pathway to enhance propulsion effectiveness while addressing stringent energy utilization requirements critical to near-space applications.

These findings underline the technical feasibility and performance advantages of tip winglet designs, offering a foundation for future research into optimizing propeller configurations for near-space and low-speed aircraft. This study contributes valuable insights into advanced aerodynamic optimization methods, with potential applications extending to a broader range of aerospace and propulsion systems.

REFERENCES

[1] Y. Gharbia, JF Derakhshandeh, MM Alam, AM Amer, Developments in Wingtip Vorticity Mitigation Techniques: A Comprehensive Review, Aerospace, 11 (2024).

[2] Z. Hui, G. Cheng, G. Chen, Experimental investigation on tip-vortex flow characteristics of novel bionic multi-tip winglet configurations, Physics of Fluids, 33 (2021).

[3] G. Mallouppas, EA Yfantis, Decarbonization in Shipping Industry: A Review of Research, Technology Development, and Innovation Proposals, Journal of Marine Science and Engineering, 9 (2021).

[4] JM Zhao, ZY Fan, M. Chang, G. Wang, Coupling Effects on Distributed Multi-Propeller Channel Wing at Low Speed Condition, Energies, 15 (2022).

[5] K. Irwin, R. Mutzman, Propeller proplet optimization based upon analytical and experimental methods, (2013).

[6] K. Oeckel, J. Heimann, M. Kerscher, S. Angermann, G. Heilmann, W. Ruther-Kindel, Comparative Acoustic Examination of UAV Propellers, in: International Congress and Exposition on Noise Control Engineering, 2018.

[7] JH Xu, WP Song, XD Yang, Effects of Proplet on Propeller Efficiency, in: American Institute of Physics Conference Series, 2011.